Preprints of the 19th World Congress
The International Federation of Automatic Control
Cape Town, South Africa. August 24-29, 2014

A Robust Model Predictive Control Framework for Diesel Generators

Timothy Broomhead * **Chris Manzie** * **Lars Eriksson** **
Michael Brear * **Peter Hield** ***

* *Department of Mechanical Engineering, The University of Melbourne, Australia (e-mail: t.broomhead@student.unimelb.edu.au).*
** *Department of Electrical Engineering, Linköping University, Sweden*
*** *Defence Science and Technology Organisation, Australia*

Abstract: A constraint tightened linear-time-varying MPC framework is proposed with applications in power tracking for variable and fixed speed generators. Current constraint tightening approaches are extended to allow for practical applications where future system representations are unknown. The resulting control structure is shown to be robustly feasible under given conditions. Knowledge about the geometry of system constraints is exploited to obtain a computationally efficient method of computing tightened sets online. A simulation study is presented demonstrating the ability of the controller to handle modelling error and demonstrate tracking of a commanded power profile.

Keywords: Predictive control, Robust Control, Engine Control, Diesel engines

1. INTRODUCTION

In applications such as diesel series hybrid electric vehicles, a high level energy management controller will typically pass down power profiles for a lower level diesel generator controller to track (Cairano et al., 2011). In addition to tracking the requested power, the controller must minimise fuel consumption whenever the target power is achievable, and at all times the generator must operate within equipment safety limits, actuator limitations and in many cases, legislative emission constraints.

For diesel generator applications, Model Predictive Control (MPC) appears an ideal candidate architecture, due to its ability to track references whilst taking into account system dynamics and explicitly handling constraints.

In many diesel engine control schemes, engine speed and fuel rate are treated as measured disturbances to the controller (Stefanopoulou et al., 2000; Wahlström and Eriksson, 2013). Where a fixed generator speed is not required, allowing speed to be a free state allows for more efficient operating points to be selected, though in some applications such as conventional diesel submarines, fixed speed generators are required. A single control formulation can serve both purposes by appropriate selection of engine speed constraints. Inclusion of both fuel rate and generator load as control inputs gives an additional degree of freedom and the option to temporarily deviate from the requested power if required to satisfy all constraints, tolerable for short periods in applications where a secondary power source can offset the error.

It is known that diesel engines exhibit strong nonlinearities (Wahlström and Eriksson, 2011), and a drawback of using MPC with nonlinear prediction models is increased computational burden. Many implementations take advantage of computationally efficient linear MPC theory by switching between a finite number of linear models which are selected based on the current operating point (Ortner and Del Re, 2007). Alternatively, a linearised form of a nonlinear model can be found at each time-step, resulting in a Linear-Time-Varying Model Predictive Control (LTV-MPC) scheme (Sharma et al., 2013). Both the switched and LTV MPC schemes suffer from model mismatch however, which can lead to infeasible solutions.

Many existing robustness techniques that deal with model mismatch, such as open or closed loop Min-Max MPC, are overly conservative or computationally intractable (Mayne et al., 2000). Constraint Tightening (CT) is introduced in Gossner et al. (1997) and further generalised by Richards and How (2006), and is a robustness technique where computational requirements generally do not exceed that of nominal robustness and robust feasibility can be guaranteed. The general principle is that constraints are systematically tightened along the horizon, effectively reserving some margin which can be used to correct for errors resulting from model mismatch at some future time. Existing formulations of CT for LTV systems assume that the system representation is known exactly in the future (Richards, 2005), which allows the tightened constraints to be calculated offline, however in an online linearisation scheme, this assumption is invalid.

This paper proposes a practical robust LTV-MPC framework with an application in power tracking for both variable and fixed speed generators subjected to constraints. Uncertainty of the internal prediction model between optimisation problems is considered and a computationally efficient form of the Pontryagin difference is proposed to permit online computation. Simulations demonstrate the capability of the resulting controller under power tracking conditions on a validated Mean Value Engine Model (MVEM).

2. MEAN VALUE ENGINE MODEL

The MVEM published in (Wahlström and Eriksson, 2011) has been utilised, with minor variations in the algebraic expressions and the addition of engine speed dynamics. The model is calibrated against data captured from a 3.0 litre direct injected diesel engine with Exhaust Gas Recirculation (EGR) and a Variable Geometry Turbocharger (VGT) commissioned at The University of Melbourne's ACART test facility. The generator is assumed to have a constant efficiency and significantly faster dynamics than the engine.

2.1 Model Description

The engine model has 7 states, $\mathbf{x} = [\omega_e, p_{im}, p_{em}, \omega_t, x_{vgt}, O_{im}, O_{em}]^T \in \Re^7$, representing engine speed, intake and exhaust manifold pressure, turbocharger speed, VGT position as well as intake and exhaust manifold oxygen fractions. The model inputs, $\mathbf{u} = [\dot{m}_f, P_{load}, u_{vgt}, u_{egr}]^T \in \Re^4$, are fuel rate (g/s), generator power (kW), VGT position demand (%) and EGR position (%). The system disturbances, $\mathbf{d} = [p_{amb}, T_{amb}, O_{amb}, p_{ex}] \in \Re^4$ are the intake pressure, temperature and oxygen content and exhaust back pressure. The dynamics are governed by

$$\dot{\omega}_e = (P_{eng}(x,u) - P_{load})/(\omega_e J_e) \tag{1a}$$
$$\dot{p}_{im} = (\dot{m}_c + \dot{m}_{egr} - \dot{m}_{ei}) R_a T_{im}/V_{im} \tag{1b}$$
$$\dot{p}_{em} = (\dot{m}_{eo} - \dot{m}_{egr} - \dot{m}_t) R_e T_{cyl}/V_{em} \tag{1c}$$
$$\dot{\omega}_t = (P_t - P_c)/(\omega_t J_t) \tag{1d}$$
$$\dot{x}_{vgt} = (u_{vgt} - x_{vgt})/\tau_{vgt} \tag{1e}$$
$$\dot{O}_{im} = [(O_{em} - O_{im})\dot{m}_{egr} + (O_{amb} - O_{im})\dot{m}_c] R_a T_{im}/(p_{im} V_{im}) \tag{1f}$$
$$\dot{O}_{em} = (O_{cyl} - O_{em})\dot{m}_t R_e T_{cyl}/(p_{em} V_{em}) \tag{1g}$$

where $J_e, V_{im}, V_{em}, J_t, \tau_{vgt}$ are tuning parameters and R_a, R_e represent the specific gas constants for intake and exhaust gases respectively. The remaining undefined terms are summarised in Table 1. Variations from the model presented in Wahlström and Eriksson (2011) are summarised as follows:

- The compressor efficiency utilises a correction for non atmospheric or time-varying inlet conditions.
- Intercoolers are assumed imperfect, with their efficiencies as functions of mass flow.
- Intake manifold temperature is a function of intercooler temperatures.
- NO rate has been included as a model output.
- Physics based models for cylinder-related sub-models are impractical for control studies. The approach taken in this work is to find correlations for these values ((2b), (5a), (5c) and (5d)) with engine states and inputs using stationary measurements, as described in Broomhead et al. (2013).

The model outputs, $\mathbf{y} = [\lambda, NO]^T \in \Re^2$, include instantaneous lambda and instantaneous NO rate (g/kWh), described as

$$\lambda = (\dot{m}_{ei} O_{im})/(AFR_s O_{amb} \dot{m}_f) \tag{2a}$$
$$NO_{\%} = [\dot{m}_f, \dot{m}_f/\omega_e, \sqrt{O2_{im}}, 1]\bar{c}_{NO} \tag{2b}$$
$$NO = \dot{m}_t NO_{\%}/P_{load} \tag{2c}$$

where AFR_s is the stoichiometric air-to-fuel ratio.

Table 1. Summary of Algebraic Expressions

Compressor

$$\Pi_c = p_{im}/p_{amb} \tag{3a}$$
$$\Psi_c = 2cp_{in} T_{amb}(\Pi_c^{(1-1/\gamma_{amb})} - 1)/(R_c^2 \omega_t^2) \tag{3b}$$
$$\Psi_1 = [\omega_t^2, \omega_t, 1]\bar{c}_{\Psi 1},\ \Phi_1 = [\omega_t^2, \omega_t, 1]\bar{c}_{\Phi 1} \tag{3c}$$
$$\Phi_c = c_{\Phi 2} + \sqrt{(max[0,\ (1 - \Psi_1(\Psi_c - c_{\Psi 2})^2)/\Phi_1]} \tag{3d}$$
$$\dot{m}_c = p_{amb}\pi R_c^3 \omega_t \Phi_c/(R_a T_{amb}) \tag{3e}$$
$$\phi_c = \dot{m}_c \sqrt{T_{amb} R_a}/p_{amb} \tag{3f}$$
$$\pi_c = (\Pi_c - 1)^{c_\pi} \tag{3g}$$
$$\eta_c = (\phi_c - c_{\phi,opt})^2 c_{c1} + (\pi_c - c_{\pi,opt})^2 c_{c2} + (\phi_c - c_{\phi,opt})(\pi_c - c_{\pi,opt}) c_{c3} \tag{3h}$$
$$P_c = \dot{m}_c cp_{in} T_{amb}(\Pi_c^{(1-1/\gamma_{amb})} - 1)/\eta_c \tag{3i}$$
$$T_c = T_{amb} + T_{amb}(\Pi_c^{1-1/\gamma_{amb}} - 1)/\eta_c \tag{3j}$$

EGR

$$\Psi_{egr} = 1 - ((1 - (p_{im}/p_{em}))/(1 - c_{egr1}) - 1)^2 \tag{4a}$$
$$A_{egr} = \left[u_{egr}, u_{egr}^2\right] \bar{c}_{egr2} \tag{4b}$$
$$\dot{m}_{egr} = A_{egr} p_{em} \Psi_{egr}/\sqrt{T_{cyl} R_e} \tag{4c}$$

Cylinders

$$M_{eng} = [\dot{m}_f \omega_e^{-1}, \omega_e, \omega_e^2, p_{em}, p_{im}, O_{im}, 1]\bar{c}_{torque} \tag{5a}$$
$$P_{eng} = \omega_e M_{eng} \tag{5b}$$
$$T_{cyl} = [\dot{m}_f \omega_e^{-1}, p_{im}^{1/2}, p_{em}, \omega_e^{1/2}, O_{im}, 1]\bar{c}_T \tag{5c}$$
$$\eta_{vol} = [p_{im}^{-1}, \omega_e, \omega_e^2, p_{im}^{-1}\omega_e^{-1}, 1]\bar{c}_{vol} \tag{5d}$$
$$\dot{m}_{ei} = (\eta_{vol} p_{im} \omega_e V_d n_{cyl})/(4\pi R_a T_{im}) \tag{5e}$$
$$\dot{m}_{eo} = \dot{m}_{ei} + \dot{m}_f \tag{5f}$$
$$O_{cyl} = (\dot{m}_{ei} O_{im} - \dot{m}_f AFR_s O_{amb})/\dot{m}_{eo} \tag{5g}$$

Intake Temperature

$$T_{ic} = T_c + (T_{amb} - T_c)[\dot{m}_c^2, \dot{m}_c, 1]\bar{c}_{\epsilon ic} \tag{6a}$$
$$T_{egr} = T_{cyl} + (T_{amb} - T_{cyl})[\dot{m}_{egr}, 1]\bar{c}_{\epsilon egrc} \tag{6b}$$
$$T_{im} = (\dot{m}_c T_{ic} + \dot{m}_{egr} T_{egr})/(\dot{m}_c + \dot{m}_{egr}) \tag{6c}$$

Turbine

$$\Pi_t = p_{ex}/p_{em} \tag{7a}$$
$$f_\Pi = \sqrt{1 - \Pi_t^{c_t}} \tag{7b}$$
$$f_{vgt} = [x_{vgt}^2, x_{vgt}, 1]\bar{c}_{vgt} \tag{7c}$$
$$\dot{m}_t = p_{em} f_\Pi f_{vgt}/\sqrt{T_{cyl} R_e} \tag{7d}$$
$$BSR = R_t \omega_t/\sqrt{2cp_e T_{cyl}(1 - \Pi_t^{1-1/\gamma_e})} \tag{7e}$$
$$\phi_m = c_{m1}(max[0, \omega_t/\sqrt{T_{cyl}} - c_{m2}])^{c_{m3}} \tag{7f}$$
$$\eta_t = c_{\eta_t} - \phi_m(BSR - c_{BSR})^2 \tag{7g}$$
$$P_t = \dot{m}_t cp_e T_{cyl}(1 - \Pi_t^{1-1/\gamma_e})\eta_t \tag{7h}$$

Nomenclature

c_x	Scalar tuning parameter
$\bar{c}_x$	Vector of tuning parameters
cp_{in}, cp_e	Isobaric specific heat of intake and exhaust gas
R_a, R_e	Specific gas constants of intake and exhaust gas
γ_{amb}, γ_e	Ratio of specific heats for intake and exhaust gas
R_c, R_t	Compressor and turbine wheel radii
AFR_s	Stoichiometric air-to-fuel ratio
n_{cyl}	Number of cylinders
V_d	Displaced volume per cylinder

3. ROBUST MPC OF AN LTV SYSTEM

3.1 Definitions

The $\sim$ operator is used to indicate the Pontryagin difference, defined as $\mathcal{A} \sim \mathcal{B} = \{\mathbf{a} \mid \mathbf{a} + \mathbf{b} \in \mathcal{A}\ \forall \mathbf{b} \in \mathcal{B}\}$ for which the property

$$c \in \mathcal{A} \sim \mathcal{B} \Rightarrow c + b \in \mathcal{A}\ \forall b \in \mathcal{B} \tag{8}$$

holds. The $\oplus$ operator describes the Minkowski sum defined as $\mathcal{A} \oplus \mathcal{B} = \{\mathbf{a}+\mathbf{b} \mid \mathbf{a} \in \mathcal{A}\ \mathbf{b} \in \mathcal{B}\}$ while the operation $\bigoplus_{i=1}^{j} \mathcal{X}_i = \mathcal{X}_1 \oplus \mathcal{X}_2 \oplus \ldots \mathcal{X}_j$ denotes the Minkowski sum of multiple sets. The symbol $\mathbb{I}_{a:b}$ denotes a vector of integers from a to b.

3.2 Internal Prediction Model

The system to be controlled is described as

$$\dot{\mathbf{x}} = \mathbf{f}(\mathbf{x}(t), \mathbf{u}(t), \mathbf{d}(t)) \tag{9a}$$
$$\mathbf{y} = \mathbf{g}(\mathbf{x}(t), \mathbf{u}(t), \mathbf{d}(t)) \tag{9b}$$

A Linear-Time-Varying (LTV) approximation of (9) can be made where at each time-step, the nonlinear model is discretised and linearised about the current state and previous control input. At time k, and assuming a constant disturbance d, this prediction model describes the system (9) as

$$\mathbf{x}_{k+1} = \mathbf{A}_k \mathbf{x}_k + \mathbf{B}_k \mathbf{u}_k + \mathbf{w}_k \tag{10a}$$
$$\mathbf{y}_k = \mathbf{C}_k \mathbf{x}_k + \mathbf{D}_k \mathbf{u}_k + \mathbf{z}_k \tag{10b}$$

where $\mathbf{w}_k$ and $\mathbf{z}_k$ accounts for modelling, discretisation and linearisation errors.

3.3 Control Development

Assumption 1. The modelling errors captured in w_k belong to a compact convex polytope $\mathcal{W}$ satisfying $0 \in \mathcal{W}$.

Assumption 2. The system (10) satisfies $\mathbf{A}_k \in \mathcal{A}, \mathbf{B}_k \in \mathcal{B}, \mathbf{C}_k \in \mathcal{C}, \mathbf{D}_k \in \mathcal{D}\ \forall k$ where sets $\mathcal{A}, \mathcal{B}, \mathcal{C}, \mathcal{D}$ are convex bounded polytopes.

Define the MPC optimisation problem, $P(k)$, as:

$$P(k) : \underset{\mathbf{u}^*, \mathbf{x}^*, \mathbf{y}^*}{\operatorname{argmin}} \sum_{j=0}^{N} \ell(\mathbf{x}_{k+j|k}, \mathbf{u}_{k+j|k}, k+j) \tag{11a}$$

subject to $\forall j \in \mathbb{I}_{0:N}$

$$\mathbf{x}_{k|k} = \mathbf{x}_k \tag{11b}$$
$$\mathbf{x}_{k+j+1|k} = \mathbf{A}_k \mathbf{x}_{k+j|k} + \mathbf{B}_k \mathbf{u}_{k+j|k} \tag{11c}$$
$$\mathbf{y}_{k+j|k} = \mathbf{C}_k \mathbf{x}_{k+j|k} + \mathbf{D}_k \mathbf{u}_{k+j|k} \tag{11d}$$
$$\mathbf{y}_{k+j|k} \in \mathcal{Y}_{k+j|k} \tag{11e}$$
$$\mathbf{x}_{k+N+1|k} \in \mathcal{X}_f \tag{11f}$$

The constraint tightening is performed as

$$\mathcal{Y}_{k|k} = \mathcal{Y} \tag{12a}$$
$$\mathcal{Y}_{k+j+1|k} = \mathcal{Y}_{k+j|k} \sim \left\{\mathcal{E}_j \oplus \mathcal{F}_j \oplus [\mathbf{C}_k + \mathbf{D}_k \mathbf{K}_{j|k}] \mathbf{L}_{j|k} \mathcal{W}\right\} \tag{12b}$$

where double indices $j|k$ denote prediction step j at time step k and $\mathbf{K}_{j|k}$ represents candidate controller matrices chosen by the practitioner. The state transition matrices $\mathbf{L}_{j|k}$ are defined as

$$\mathbf{L}_{j|k} = \begin{cases} \mathbf{0} & j < 0 \\ \mathbf{I} & j = 0 \\ (\mathbf{A}_k + \mathbf{B}_k \mathbf{K}_{j-1|k}) \mathbf{L}_{j-1|k} & j > 0 \end{cases}$$

Assumption 3. There exists a control law $\kappa(\mathbf{x})$ such that the terminal set $\mathcal{R}$ is a control invariant admissible set satisfying $\forall \mathbf{x} \in \mathcal{R}, \forall k$

$$\mathbf{A}_k \mathbf{x} + \mathbf{B}_k \kappa(\mathbf{x}) + \mathbf{L}_{N|k} \mathbf{w} \in \mathcal{R}, \forall \mathbf{w} \in \mathcal{W} \tag{13a}$$
$$\mathbf{C}_k \mathbf{x} + \mathbf{D}_k \kappa(\mathbf{x}) \in \mathcal{Y}_{k+N|k} \tag{13b}$$

Assumption 4. Sets $\mathcal{R}$ ans $\mathcal{Y}$ are sufficiently large with respect to $\mathcal{W}$ such that after tightening, the resulting constraint sets are non-empty.

Remark 2. Output constraint (11e) can capture state, input and input rate constraints by appropriate augmentation of matrices $\mathbf{A}, \mathbf{B}, \mathbf{C}$ and $\mathbf{D}$ and state vector $\mathbf{x}$.

Remark 3. This formulation is distinct from CT-LTV controller detailed in (Richards, 2005), in particular

(1) At each time-step the LTV system (10) is linear-time-invariant across the prediction horizon.
(2) The system representation $\mathbf{A}$, $\mathbf{B}$, $\mathbf{C}$ and $\mathbf{D}$ are not known in advance.
(3) The point terminal constraint is replaced with a set.

Theorem 1. (Robust Feasibility). Under Assumptions 1-4, sets $\mathcal{F}_j, \mathcal{E}_j$ and $\mathcal{X}_f$ exist such that if P(0) has a feasible solution then subsequent optimisations $P(k)$ are robustly feasible $\forall k > 0$.

Proof. This proof follows from (Richards, 2005; Richards and How, 2006) and is based on recursion, showing that feasibility of $P(k_0)$ implies feasibility of $P(k_0 + 1)$. Feasibility of $P(k_0 + 1)$ is proven by showing the existence of a solution which obeys all constraints (11). Assume a feasible solution exists for problem $P(k_0)$, denoted by $\mathbf{u}^*$ with corresponding output and state trajectories $\mathbf{y}^*$ and $\mathbf{x}^*$. Variables marked by $\hat{\cdot}$ denote the respective analogues for problem $P(k_0 + 1)$. Consider the following candidate control sequence

$$\hat{\mathbf{u}}_{k_0+1+j} = \mathbf{u}^*_{k_0+1+j} + \mathbf{K}_{j|k_0+1} \mathbf{L}_{j|k_0+1} \mathbf{w}_{k_0} \quad \forall j \in \mathbb{I}_{0:N-1} \tag{14a}$$
$$\hat{\mathbf{u}}_{k_0+1+N} = \kappa(\hat{\mathbf{x}}_{k_0+1+N}) \tag{14b}$$

The initial condition, dynamic constraints and output equality constraints are satisfied by construction. Feasibility of $P(k_0)$ implies $\mathbf{x}^*_{k_0+1} = \mathbf{A}_{k_0} \mathbf{x}_{k_0} + \mathbf{B}_{k_0} \mathbf{u}_{k_0}$, substitution into system dynamics (10) gives $\mathbf{x}_{k_0+1} = \mathbf{x}^*_{k_0+1} + \mathbf{w}_{k_0}$. Using this initial condition and proposed control sequence (14), the dynamic constraint (11c) gives the following state sequence $\forall j \in \{0, \ldots, N\}$ at time k_0+1, expressed relative to the solution at time k_0

$$\hat{\mathbf{x}}_{k_0+1+j} = \mathbf{x}^*_{k_0+1+j} + \mathbf{L}_{j|k_0+1} \mathbf{w}_{k_0} + \mathbf{m}_{j|k_0} \forall j \in \mathbb{I}_{0:N} \tag{15}$$

where

$$\mathbf{m}_{0|k} = \mathbf{0} \tag{16a}$$
$$\mathbf{m}_{j|k} = \mathbf{A}_{k+1} \mathbf{m}_{j-1|k} + (\mathbf{A}_{k+1} - \mathbf{A}_k) \mathbf{x}^*_{k+j} + (\mathbf{B}_{k+1} - \mathbf{B}_k) \mathbf{u}^*_{k+j} \tag{16b}$$

and similarly (11d) gives output sequence

$$\hat{\mathbf{y}}_{k_0+1+j} = (\mathbf{C}_{k_0+1} + \mathbf{D}_{k_0+1} \mathbf{K}_{j|k_0+1}) \mathbf{L}_{j|k_0+1} \mathbf{w}_{k_0} + \mathbf{y}^*_{k_0+1+j} + \mathbf{e}_{j|k_0} \forall j \in \mathbb{I}_{0:N-1} \tag{17a}$$
$$\hat{\mathbf{y}}_{k_0+1+N} = \mathbf{C}_{k_0+1} \hat{\mathbf{x}}_{k_0+1+N} + \mathbf{D}_{k_0+1} \kappa(\hat{\mathbf{x}}_{k_0+1+N}) \tag{17b}$$

where

$$\mathbf{e}_{j|k} = (\mathbf{C}_{k+1} - \mathbf{C}_k)\mathbf{x}^*_{k+1+j} + (\mathbf{D}_{k+1} - \mathbf{D}_k)\mathbf{u}^*_{k+1+j} + \mathbf{C}_{k+1}\mathbf{m}_{j|k} \quad (18)$$

If the set $\mathcal{F}_j$ is chosen to satisfy $\forall k$

$$\bigoplus_{i=1}^{j}([\mathbf{C}_{k+1} + \mathbf{D}_{k+1}\mathbf{K}_{i|k+1}]\mathbf{L}_{i|k+1} - [\mathbf{C}_k + \mathbf{D}_k\mathbf{K}_{i|k}]\mathbf{L}_{i|k})\mathcal{W} \subseteq \mathcal{F}_j \quad (19)$$

then comparison of (12b) for successive time steps gives

$$\mathcal{Y}_{k_0+1+j|k_0} \subseteq \mathcal{Y}_{k_0+1+j|k_0+1} \sim (\mathcal{E}_j \oplus [\mathbf{C}_{k_0+1+j} + \mathbf{D}_{k_0+1+j}\mathbf{K}_{j|k_0}]\mathbf{L}_{j|k_0}\mathcal{W}) \quad (20)$$

furthermore, if $\mathcal{E}_j$ is chosen to satisfy

$$\mathbf{e}_{j|k} \in \mathcal{E}_j \ \forall k \quad (21)$$

then substitution of and (17a) and (20) into the property (8) shows that under Assumptions 1,2,4 if $\mathbf{y}^*_{k_0+j+1} \in \mathcal{Y}k_0 + 1 + j|k_0$, which is known due to feasibility at time k_0 then $\hat{\mathbf{y}}_{k_0+j+1} \in \mathcal{Y}_{k_0+1+j|k_0+1}$, satisfying the constraint (11e) for $j \in \mathbb{I}_{0:N-1}$ at time $k_0 + 1$. Define the terminal constraint set as

$$\mathcal{X}_f = \mathcal{R} \sim L_N\mathcal{W} \sim \mathcal{M} \quad (22)$$

where $\mathbf{m}_{N|k} \in \mathcal{M}\ \forall k$. Feasibility at time k_0 also requires $\mathbf{x}^*_{k_0+1+N} \in \mathcal{X}_f$ and hence (22) and (15) imply $\hat{\mathbf{x}}_{k_0+1+N} \in \mathcal{R}$. Then under Assumption 3 the requirements on $\mathcal{R}$ guarantee that the output (17b) satisfies $\hat{\mathbf{y}}_{k_0+1+N} \in \mathcal{Y}_{N|k_0+1}$, hence all output constraints are satisfied.

Finally the terminal constraints must be satisfied at time $k_0 + 1$. The new terminal state is found by substituting the candidate control (14b) into the dynamics constraint

$$\hat{\mathbf{x}}_{k_0+N+2} = \mathbf{A}_{k_0+1}\hat{\mathbf{x}}_{k_0+1+N} + \mathbf{B}_{k_0+1}\kappa(\hat{\mathbf{x}}_{k_0+1+N}) \quad (23)$$

since it has already been shown that $\hat{\mathbf{x}}_{k_0+1+N} \in \mathcal{R}$ and $\mathcal{R}$ is a robustly control invariant set following from Assumption 3, then the new state satisfies $\hat{\mathbf{x}}_{k_0+N+2} + \mathbf{L}_N\mathbf{w}_{k_0} + \mathbf{m}_{N|k_0} \in \mathcal{R}$ which together with the definition (22) implies $\hat{\mathbf{x}}_{k_0+N+2} \in \mathcal{X}_f$, completing satisfaction of all constraints at $k_0 + 1$. Hence the proposed sets $\mathcal{X}_f, \mathcal{E}_j$ and $\mathcal{F}_j$ combined with feasibility at k_0 guarantees feasibility at $k_0 + 1$, and through recursion $\forall k > k_0$. □

Remark 4. The choice of sets (19),(21) and (22) show that recursive feasibility can exist, however they depend on the choice of (14) and hence are not unique.

Remark 5. Theorem 1 guarantees the optimisation problem is recursively feasible and hence the predicted outputs do not violate the constraints along the horizon. To ensure that the real system (9) does not violate output constraints, the output constraint set $\mathcal{Y}$ in (12a) should be replaced with $\mathcal{Y} \sim \mathcal{Z}$ where $\mathbf{z}_k \in \mathcal{Z}\ \forall k$.

3.4 Practical Set Determination

Since $\mathcal{X}_f, \mathcal{E}$ and $\mathcal{F}$ cannot always be calculated explicitly in advance, a practical approach to finding appropriate sets is required. Under Assumption 2 an upper bound for the sets exists. However, for systems which evolve slowly, this upper bound will be overly conservative and may lead to violation of Assumption 4. Furthermore, following from Remark 4, the definitions of the sets used in the proof for Theorem 1 may already be conservative.

The sets are therefore suggested to be found empirically through a Monte Carlo approach to find typical values of $\mathbf{A}, \mathbf{B}, \mathbf{C}, \mathbf{D}$ and terms $\mathbf{e}$ and $\mathbf{m}$ for a given application. Removing outlier points using confidence bounds on the empirical data results in reduced conservativeness and may avoid violation of Assumption 4. This method may result in absolute guarantees for robustness being lost, however the simulation study presented in Section 4 demonstrates sensible selection of confidence bounds resulting in practical robustness.

3.5 Practical Calculation of Pontryagin Difference

Proposition 1. Given that a set $\mathcal{A} = \{a : a_{lb} \leq a \leq a_{ub}\}$, representing an orthotope, is being tightened by a set $\mathcal{B}$ using the Pontryagin difference, then $\mathcal{B}$ can be approximated by $\mathcal{C} = \{c : min(\mathcal{B}) \leq c \leq max(\mathcal{B})\}$, the smallest bounding orthotope to fully contain $\mathcal{B}$ and the resulting set will be unchanged. Note: *min* and *max* represent element-wise operations.

Remark 7. The Pontryagin difference of sets $\mathcal{A} = \{a : a_{lb} \leq a \leq a_{ub}\}$ and $\mathcal{B} = \{b : b_{lb} \leq b \leq b_{ub}\}$ can be trivially found, where $A \sim B = \{c : a_{lb} - b_{lb} \leq c \leq a_{ub} - b_{ub}\}$.

Calculating the Pontryagin difference of sets multiple times at each timestep, may not be computational tractable in an online environment. Use of Proposition 1 and Remark 7 in cases where the original constraint sets can be represented by orthotopes results in the Pontryagin difference calculation being small in computation time compared to solving the optimisation problem, as found in the simulation study presented in Section 4.

4. SIMULATION STUDY

All simulations utilise the full order and validated model (1) and (2) to represent the engine. Optimisation setup is performed in an interpreted Matlab (v. 2013a) script while the optimisation is performed by qpOASES (Ferreau et al., 2008), on a 4-core $2.7GHz$ Intel i5 processor.

An explicit form of the linearisation of (1) and (2) was found with the aid of the Matlab Symbolic Toolbox. The algebraic expressions (3d) and (7f) contain switches, therefore a total of 4 linearisations of (1)-(2) are used, one for each permutation of the cases. The switches are evaluated online, and the appropriate linearisation selected at each time-step. The controller's robustness is demonstrated with modelling error arising between the linear-time-varying discrete time model and the simulated continuous time MVEM.

4.1 Controller Formulation

In order to meet the objectives described in Section 1 the following cost function which penalises power tracking error and fuel use can be used for (11a)

$$\ell = \delta(P_{load}(k+j|k) - P_{ref}(k+j))^2 + \dot{m}_f(k+j|k)^2 \quad (24)$$

where δ represents the relative weighting between power tracking and fuel minimisation. This choice of cost function is atypical in that only input terms are penalised. However in generator applications the outputs must only satisfy safe operating conditions, which can be specified by appropriate constraints. Since these terms are quadratic, the resulting optimisation can be formulated

Table 2. Lower and Upper Constraints

Bounds	ω_e (rpm)	$\dot{m}_f$ (g/s)	u_{vgt} (%)	u_{egr} (%)	Δu_{egr} (%)	Δu_{vgt} (%)	NO (g/kWh)	λ
Lower	1500	1	60	0	-5	-4	-	1.3
Upper	2500	5	90	100	5	4	5.5	-

Note: The NO rate limitation is not directly comparable to, for example, the Euro emissions standards, as these constraint NO_x.

as a quadratic program (QP). A time-step of 100 ms has been chosen. The power request is comprised of a number of randomly generated step changes between $25kW$ and $70kW$, which spans the range of calibration data for the engine, representing an aggressive test case.

Representative emission constraints are comprised of a maximum averaged Nitrogen Monoxide rate (NO) g/kWh and a minimum instantaneous lambda (normalised air-fuel ratio) to prevent excessive Particulate Matter (PM) emissions. These output constraints are represented by simple bounds, $[\mathrm{NO},\ -\lambda]^T \leq [\bar{\mathrm{NO}},\ \bar{\lambda}]^T$ where $\bar{\mathrm{NO}}$ and $\bar{\lambda}$ are chosen by system designers. Engine speed limits are described by $\omega_{e,ub} \leq \omega_e \leq \omega_{e,ub}$. Each of the engine inputs are constrained by simple bounds, $u_{lb} \leq u \leq u_{ub}$, representing actuator limits. In addition, input rate limitations are enforced for EGR and VGT actuators, $\Delta u_{lb} \leq u_k - u_{k-1} \leq \Delta u_{ub}$, representing actuator slew rate limits.

Taking into account these constraints, summarised in Table 2, applying large bounds designed never to be active on any unbounded values, and following from Remark 2, the constraints (12a) can be put into sets of the form $\mathcal{Y} = \{y : y_{lb} \leq y \leq y_{ub}\}$ which geometrically represent orthotopes, allowing Proposition 1 to be utilised. The terminal constraint set (11f) is chosen as $\mathcal{X}_f = \{x_f : x_{f,lb} \leq x_f \leq x_{f,ub}\}$, where $x_{f,lb}, x_{f,ub}$ are assumed to be conservative.

There is no requirement for tuning the candidate control function to guarantee robustness of (11) under Assumptions 1-4. A nilpotent LQR controller was chosen with $Q = I_7$, $R = I_4$ and $M = 5$ (Richards, 2005, Sec. III).

The sets $\mathcal{W}, \mathcal{E}_j$, and $\mathcal{F}_j$ $\forall j \in \mathbb{I}_{1:N}$ required by (12) are calculated according to the method described in Section 3.4. The MPC controller is set to track a random power trajectory for $60s$, initiated using manually chosen tightening sets to generate the appropriate data. The set $\mathcal{W}$ was selected to be the largest orthotope to contain all calculated $\mathbf{w}$ values for the simulation within 1st and 99th percentiles, while the remaining sets are the smallest orthotopes to contain all respective values within 3rd and 97th percentiles. Setting the tightening sets to be empty sets resulted in infeasible optimisations during the simulation, whilst making the confidence bounds too large resulted in infeasible solutions at $k = 0$ due to violation of Assumption 4.

It is particularly important that the instantaneous lambda constraint is not violated, as this may result in excessive PM production and undesirable visible smoke. However, it is the average g/kWh of NO produced over a drive cycle that is typically critical, and so temporary violation of the instantaneous NO constraint is acceptable. As such Remark 5 is taken into consideration for the lambda constraint only, where $\mathcal{Z}$ is calculated with the same method as used to find $\mathcal{W}$.

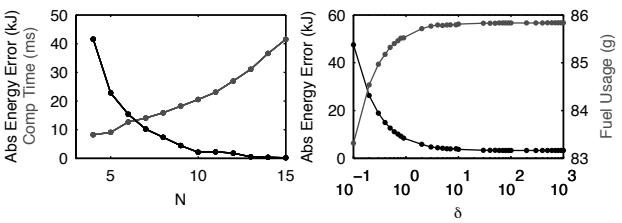

Fig. 1. Left: Absolute energy error and computation time with varying N Right: Impact on absolute energy error and fuel use with changing δ

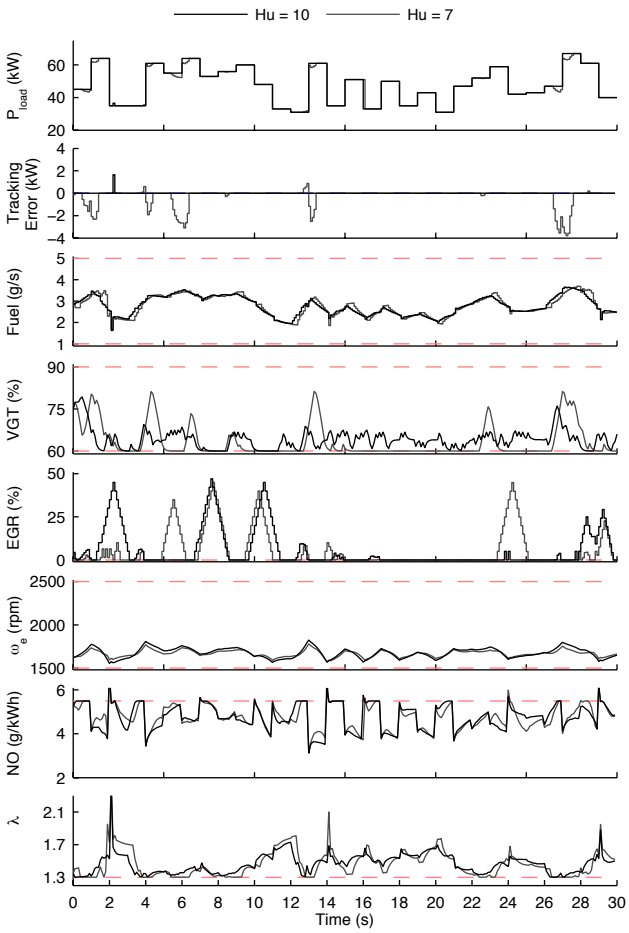

Fig. 2. Simulated diesel engine under LTV MPC schemes

To satisfy the objectives of Section 1, δ in (24) should be large, so that fuel minimisation only strongly influences the cost function when power tracking is first satisfied. Figure 1 shows the tracking error and fuel consumption of a 30 second simulation of the controller following the same power trajectory for varying δ where $N = 10$. As δ increases, the performance of the controller converges to a single solution, indicating that δ can be made arbitrarily large, reducing tuning requirements, though numerical tolerances of the solver should be considered.

4.2 Controller Performance

Figure 2 illustrates the performance of the controller for 30 seconds of a power request with $\delta = 100$ and $N \in \{7, 10\}$. For longer horizon lengths, power tracking using

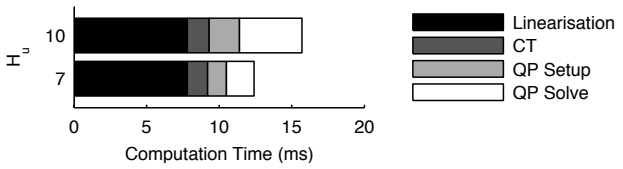

Fig. 3. Computation time for varying prediction horizons

this formulation is shown to be almost perfect, while fuel minimisation is apparent from the relatively low VGT positions and engine speeds. The extra degree of freedom allowed by including generator load as a control input is utilised for short periods, particularly for shorter horizon lengths, where power tracking performance is sacrificed in order to ensure compliance with constraints.

Figure 1 highlights the trade-off between power tracking and computational requirements for a 30 second simulation of the controller by varying N where $\delta = 100$. The median computation time shown includes linearisation, constraint tightening, and solving the QP. Increasing the horizon length generally increases the tracking performance, though with diminishing returns and increased computation requirements.

A breakdown of computational expense is presented in Figure 3 for the two controllers presented in Figure 2. Due to the use of Proposition 1, the cost of calculating the tightened sets online is smaller than both linearisation and solving the optimisation. The large expense in linearisation comes due to the integration technique required due to the system (1),(2) being stiff. For the horizon lengths shown, the results indicate that computation times are compatible with online control where a timestep of $100ms$ is used. However, this framework's ability to handle modelling error lends itself to use of model reduction such as that presented in Sharma et al. (2011) to further reduce the computational cost.

5. CONCLUSION / FURTHER WORK

An extension to CT techniques has been presented to explicitly take into account additional uncertainty in internal prediction models, facilitating integration of CT techniques with existing online LTV-MPC schemes. Online computation of the resulting controller is made feasible by utilising knowledge about the structure of constraints. The extensions allow the use of CT in practical applications, as demonstrated by way of simulation example. Future work will focus on experimental validation and further reduction of computational requirements through model reduction.

ACKNOWLEDGMENTS

The authors would like to thank the Defence Science and Technology Organisation Australia, the Defence Science Institute Australia and the Elizabeth and Vernon Puzey trust for their support of this research.

REFERENCES

Broomhead, T., Manzie, C., Brear, M., Hield, P., Tregenza, O., and Newman, M. (2013). Control oriented modelling of submarine diesel engines. In *Proc. of the ACS*.

Cairano, S.D., Liang, W., Kolmanovsky, I.V., Kuang, M.L., and Phillips, A.M. (2011). Engine power smoothing energy management strategy for a series hybrid electric vehicle. In *Proceedings of the ACC*.

Ferreau, H.J., Bock, H.G., and Diehl, M. (2008). An online active set strategy to overcome the limitations of explicit MPC. *Int. J. Robust Nonlin. Contr.*, 18(8), 816–830.

Gossner, J., Kouvaritakis, B., and Rossiter, J.A. (1997). Stable generalized predictive control with constraints and bounded disturbances. *Automatica*, 33(4), 551–568.

Mayne, D.Q., Rawlings, J.B., and Scokaert, C. (2000). Constrained model predictive control: Stability and optimality. *Automatica*, 36, 789–814.

Ortner, P. and Del Re, L. (2007). Predictive control of a diesel engine air path. *IEEE Trans. CST*, 15(3), 449–456.

Richards, A. (2005). Robust model predictive control for time-varying systems. In *IEEE Conf. on Decis. and Contr.*, 3747–3752.

Richards, A. and How, J. (2006). Robust stable model predictive control with constraint tightening. In *Proc. of Amer. Contr. Conf.*, 1557–1562.

Sharma, R., Nesic, D., and Manzie, C. (2011). Model reduction of turbocharged (TC) spark ignition (SI) engines. *IEEE Trans. CST*, 19(2), 297–310.

Sharma, R., Nesic, D., and Manzie, C. (2013). Sampled data model predictive idle speed control of ultra-lean burn hydrogen engines. *IEEE Trans. CST*, 21(2), 538–545.

Stefanopoulou, A.G., Kolmanovsky, I., and Freudenberg, J.S. (2000). Control of variable geometry turbocharged diesel engines for reduced emissions. *IEEE Trans. CST*, 8(4), 733–745.

Wahlström, J. and Eriksson, L. (2011). Modelling diesel engines with a variable-geometry turbocharger and exhaust gas recirculation by optimization of model parameters for capturing nonlinear system dynamics. *J. of Automob. Eng.*, 225(7), 960.

Wahlström, J. and Eriksson, L. (2013). Output selection and its implications for MPC of EGR and VGT in diesel engines. *IEEE Trans. CST*, 21(3), 932–940.